Sub-ns Switching and Cryogenic-Temperature Performance of Mo-Based Perpendicular Magnetic Tunnel Junctions

Deyuan Lyu, *Graduate Student Member, IEEE*, Pravin Khanal, Yang Lv, Bowei Zhou, Hwanhui Yun, Qi Jia, *Graduate Student Member, IEEE*, Brandon R. Zink, Yihong Fan, K. Andre Mkhoyan, Weigang Wang, *Member, IEEE*, and Jian-Ping Wang, *Fellow, IEEE*

***Abstract*— Mo-based perpendicular magnetic tunnel junctions (Mo-pMTJs) can outperform mainstream Ta-pMTJs in terms of perpendicular magnetic anisotropy (PMA) and thermal tolerance. However, studies on the ultrafast switching of Mo-pMTJ devices remain limited. In addition, although pMTJ devices have potential to function as cryogenic memory cells, there has been no report on the performance of Mo-pMTJs at low temperatures until now. In this Letter, Mo-pMTJs were prepared with strong PMA and patterned into nanoscale devices. Scanning transmission electron microscopy was employed to characterize the device lateral dimension and structure integrity. Systematic probability measurements were conducted under various pulse widths and current densities. On the ultrafast timescale down to sub-ns, the switching is confirmed to enter the precessional regime. The optimization of the switching energy is discussed. Moreover, we investigate the magneto-transport properties and switching of Mo-pMTJs at low temperatures down to 2 K. The feasibility of utilizing Mo-pMTJ devices in cryogenic memory is verified through this work.**

Manuscript received 13 May 2022; revised 10 June 2022; accepted 15 June 2022. Date of publication 17 June 2022; date of current version 26 July 2022. This work was supported in part by the Defense Advanced Research Projects Agency (DARPA) (Advanced MTJs for computation in and near random access memory) under Grant HR001117S0056-FP-042, in part by the Minnesota Nano Center by the National Science Foundation through the National Nanotechnology Coordinated Infrastructure (NNCI) under Award ECCS-2025124, and in part by the Characterization Facility of University of Minnesota by National Science Foundation (NSF) through the UMN MRSEC (for the electron microscopy work) under Grant DMR-2011401. The work of Hwanhui Yun and K. Andre Mkhoyan was supported by the MRSEC Program DMR-2011401 and SMART, one of seven centers of nCORE, a Semiconductor Research Corporation Program, sponsored by National Institute of Standards and Technology (NIST). The review of this letter was arranged by Editor B. G. Malm. *(Corresponding authors: Jian-Ping Wang; Weigang Wang.)*

Deyuan Lyu, Yang Lv, Qi Jia, Brandon R. Zink, Yihong Fan, and Jian-Ping Wang are with the Department of Electrical and Computer Engineering, University of Minnesota, Minneapolis, MN 55455 USA (e-mail: jpwang@umn.edu).

Pravin Khanal, Bowei Zhou, and Weigang Wang are with the Department of Physics, The University of Arizona, Tucson, AZ 85721 USA (e-mail: wgwang@arizona.edu).

Hwanhui Yun and K. Andre Mkhoyan are with the Department of Chemical Engineering and Materials Science, University of Minnesota, Minneapolis, MN 55455 USA.

Color versions of one or more figures in this letter are available at https://doi.org/10.1109/LED.2022.3184278.

Digital Object Identifier 10.1109/LED.2022.3184278

***Index Terms*— Molybdenum (Mo), perpendicular magnetic tunnel junctions, sub-ns switching, cryogenic memory.**

I. Introduction

OVER the past decade or so, magnetic tunnel junctions with perpendicular easy axis (pMTJs) have attracted continuous attention owing to their lower switching energy, higher speed, better scalability [1]–[4], and therefore, better application prospects than the in-plane magnetized counterparts. The most extensively studied pMTJ material system is Ta|CoFeB|MgO [4], [5], where Ta functions as the buffer/cap of the CoFeB electrodes and promotes their perpendicular magnetic anisotropy (PMA) under proper post-annealing. Specifically, B atoms diffuse out of CoFeB and into Ta upon annealing, leaving CoFe crystalized and strongly bonded to O at CoFe(B)|MgO interfaces [6], at which interfacial PMA is thus generated [7], [8]. However, the PMA of Ta-based pMTJs (Ta-pMTJs) is usually insufficient (1–2 mJ/m^2), especially after the high-temperature processing required by CMOS technologies, to provide a high thermal stability for advanced technical nodes [9]. Thus, substantial efforts have been made to develop alternative buffer/cap materials, including W [10], [11], Mo [12], [13], *et al.* [14]–[16]

Among all emerging candidates, Mo-pMTJs are outstanding, attributing to their high PMA and excellent thermal tolerance. In 2015, we demonstrated enhanced PMA and tunnel magnetoresistance (TMR) in Mo-pMTJs than Ta-pMTJs [12]. A materials design framework, proposed in 2019, also predicates higher PMA in Mo|CoFeB|MgO than that in Ta|CoFeB|MgO, and guided the experimental demonstration of reasonably good PMA of 1.74 mJ/m^2 in samples annealed above 400°C [17]. In 2020, a remarkably large PMA of 4.06 mJ/m^2 was reported in Mo-based double-interface free layers, in contrast to lower than 3 mJ/m^2 in Ta-and W-based counterparts [18]. In our most recent study, strong PMA and large TMR ratios up to 212% were achieved in pMTJs with 2–100 μm diameters using Mo-based multi-interface free layers [19]. In addition, lower Gilbert damping constants, which are in favor of increasing switching speed and decreasing power consumption, were obtained very recently in Mo-pMTJs and related thin films compared with W-based ones [20].

Despite the rapid progress in the layer structure and magnetic performance, ultrafast switching of Mo-pMTJs is rarely

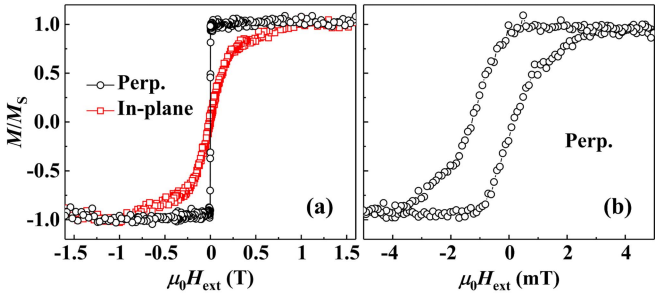

Fig. 1. (a) The magnetic hysteresis loops of the Mo-pMTJ stack under perpendicular and in-plane $\mu_0 H_{ext}$. (b) The low-field region with perpendicular $\mu_0 H_{ext}$.

reported. To our knowledge, the fastest ever reported switching of Mo-pMTJs is 10–1000 ns [21], in which the switching behavior still follows the thermal activation mode or its transition to the precessional switching mode. To become sufficiently competitive to replace DRAM or even SRAM, pMTJ devices must support ultrahigh switching speeds faster than 1 ns, where the precessional switching mode dominates [22]. Furthermore, the functionality of W-pMTJs at 4 K was demonstrated in 2019 [23], making pMTJ devices potential cryogenic memory cells serving in superconducting circuits [24]. However, the cryogenic-temperature functionality of Mo-pMTJ devices has yet to be tested.

In this Letter, we first fabricate Mo-pMTJs and subsequently characterize the magnetic performance at the film-level as well as the lateral dimension and structure integrity at the device-level. Then, we study the spin-transfer torque (STT)-driven switching of Mo-pMTJs on an ultrafast timescale down to sub-ns, where the precessional switching is observed. The optimal switching energy for both parallel-to-antiparallel (P→AP) and AP→P switching are analyzed. Moreover, we investigate the temperature (T)-dependence of the magneto-transport properties and switching of Mo-pMTJ devices, at $T = 300-2$ K. Our work shows the potential of Mo-pMTJs for cutting-edge applications.

II. Device Fabrication and Characterization

The Mo-pMTJ stack with a core layer structure of Mo 12|$Co_2Fe_6B_2$ 10|MgO 9|$Co_2Fe_6B_2$ t_{CFB}|Mo 19 (unit: Å), where t_{CFB} is wedged 12−15 Å, was deposited by magnetron sputtering and annealed at 300°C for 20 min. More fabrication details are described in our earlier report [12]. Fig. 1(a) shows the magnetic hysteresis (magnetization (M) vs $\mu_0 H_{ext}$) loops, measured by vibrating-sample magnetometry (VSM), of the stack under perpendicular and in-plane $\mu_0 H_{ext}$, where μ_0 is the vacuum permeability and H_{ext} denotes the external magnetic field. The low-field region with perpendicular $\mu_0 H_{ext}$ is additionally shown in Fig. 1(b). At $t_{CFB} \approx 15$ Å, the areal saturation magnetization (M_S) is about 2.20 mA. The stack shows apparent PMA with a large in-plane anisotropy field of ~ 1 T.

Using e-beam lithography and Ar^+ ion milling, we patterned the films into circular nanopillar devices. The device cross-section was cut by using the focused ion beam technique and imaged using the annular bright-field mode of scanning transmission electron microscopy (STEM), as shown in Fig. 2(a). The lateral dimension (i.e., device diameter) is estimated to be 100 nm. The energy dispersive X-ray (EDX) elemental maps (Figs. 2(b-d)) were acquired from one selected region (yellow dash line) in Fig. 2(a), showing that the

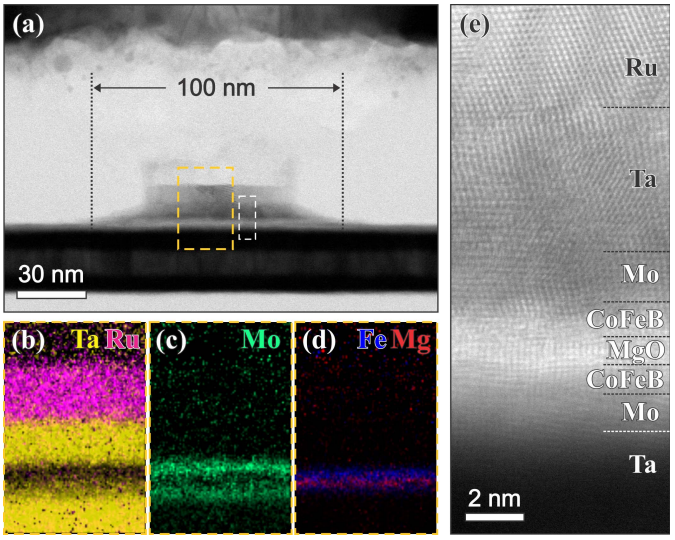

Fig. 2. (a) The cross-sectional STEM image of a Mo-pMTJ device. (b), (c), and (d) The EDX elemental maps of one selected region (yellow dash line) in (a). (e) The atomic-resolution STEM image of the other selected region (white dash line).

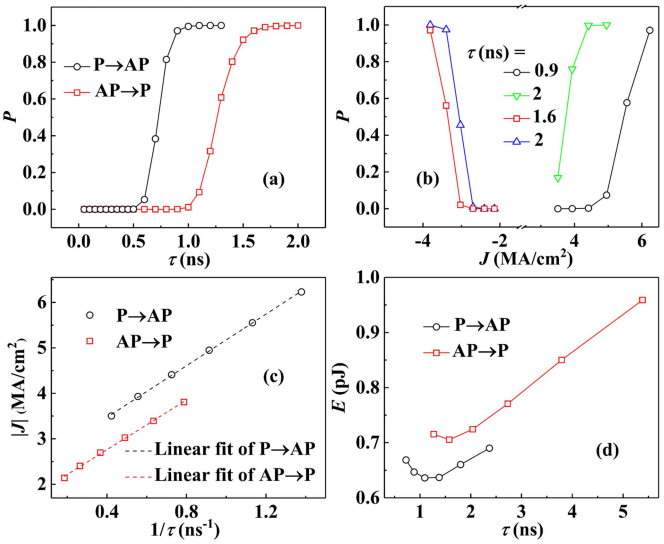

Fig. 3. (a) and (b) P as a function of τ and J, respectively. At $P = 0.5$, (c) J as a function of $1/\tau$, and (d) E as a function of τ. Measurements were conducted at room temperature.

Mo-pMTJ device is well-structured and intact after annealing and patterning. Fig. 2(e) is an atomic-resolution STEM image of the other selected region (white dash line) and presents good crystallinity of MgO and CoFeB layers.

The switching probability (P), calculated from 11,000 trials per each value, was measured at room temperature as a function of the pulse width (τ) and current density (J) by the same measurement setup reported in our previous study [25]. All the T-dependent tests were conducted with a Physical Property Measurement System (PPMS). A bias field of 36–38 mT was applied during the tests to cancel the stray fields. Unless specified, all the results were collected from the central part ($t_{CFB} \approx 13.5$ Å) of the sample.

III. Ultrafast Switching and Analysis

As shown in Fig. 3(a), switching boundaries (i.e., $P = 0.5$) at roughly $\tau = 0.75$ ns (P→AP) and 1.3 ns (AP→P) are

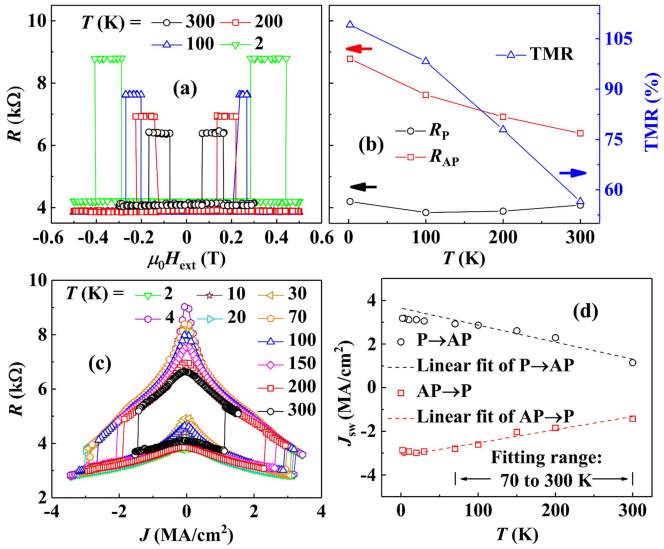

Fig. 4. (a) Major R vs $\mu_0 H_{ext}$ loops at different T. (b) R_P, R_{AP}, and TMR as functions of T. (c) R vs J loops under quasistatic currents at different T. (d) The T-dependence of J_{sw}.

realized. Further decreasing τ (i.e., increasing J) will induce dielectric breakdown during the 11,000 trials. At $\tau = 0.9$ ns, as presented in the right half of Fig. 3(b), $J = 6$ MA/cm^2 can drive P→AP switching with a close-to-complete P of more than 0.97. To avoid dielectric breakdown, $\tau = 1.6$ ns is needed to reach the same P for AP→P switching (left half of Fig. 3(b)) with $J = -4$ MA/cm^2 as the AP state possesses higher junction resistance. The P of both switching directions at $\tau = 2$ ns are also plotted in Fig. 3(b), which shows that lower J is needed for the ultrafast AP→P switching, reflecting the asymmetric nature of the STT mechanism [26].

To further investigate the switching behavior on the ultrafast timescale, the J that corresponds to $P = 0.5$ is plotted in Fig. 3(c) as a function of $1/\tau$. Linear relationships in both switching directions are evident, indicating a precessional switching mode where τ is inversely proportional to $J - J_{C0}$ [22], where J_{C0} is the intrinsic critical switching current density. Linear fit yields $J_{C0} = 2.34$ MA/cm^2 (P→AP) and 1.67 MA/cm^2 (AP→P), respectively.

The switching energy (E) is of critical importance for memory and logic applications. We calculate E (at $P = 0.5$) using the equation $E = V^2\tau/R$, where V is the applied voltage, R represents the device resistance and is taken before switching. Fig. 3(d) shows that, as τ decreases, E first decreases and then increases, which agrees with our previous study on in-plane magnetized devices [27]. Consequently, we can optimize E by tuning τ. In this study, the optimal E is determined to be 0.64 pJ/bit (P→AP) and 0.71 pJ/bit (AP→P), which occurs at $\tau = 1.09$ ns and 1.58 ns, respectively. It is worth mentioning that although a higher J is required in P→AP switching, both R and τ are smaller than those of AP→P switching. As a result, we obtained lower E in P→AP switching, because E is proportional to $J^2 R\tau$.

IV. Device Performance at Cryogenic Temperatures

Representative major R vs $\mu_0 H_{ext}$ loops at different T are plotted in Fig. 4(a). As T decreases, the switching field and R in AP state (R_{AP}) increase significantly, while R_P is less T-dependent, which is consistent with earlier results [28]–[31]. R_{AP}, R_P, and TMR ratios, defined by $100\% \times (R_{AP} - R_P)/R_P$, at different T are summarized in Fig. 4(b). Due to the steady increase of R_{AP}, the TMR ratio is enhanced from 56.5% to 109.1% as T decreases from 300 K to 2 K. It is noteworthy that with a slightly thicker $t_{CFB} \approx 14$ Å (not shown here) the TMR ratio significantly increases to $> 100\%$ at room temperature and $> 200\%$ at 30 K due to the higher spin polarization.

In addition, we measured the R vs J loops at various T. As shown in Fig. 4(c), STT switching is observed at all T, which demonstrates the cryogenic functionality of Mo-pMTJs. The bias-dependence of R_{AP}, R_P, and TMR under various T are in agreement with early results [32]. In general, the switching current density J_{sw} increases as T decreases, as summarized in Fig. 4(d). Nonetheless, at deeply low T, like 20 K, J_{sw} for both switching directions are almost independent of T. This can be explained by the thermal effect of Joule heating, which increases the local junction temperature [33].

Fig. 4(d) also shows the linear fit of J_{sw} vs T that samples in the range of 300−70 K, but is extended to 2 K. For P→AP switching, J_{sw} noticeably deviates from the fit and barely changes below 30 K. For AP→P switching, the J_{sw} at 30 K and 20 K seem to follow the fit. Further lowering T, however, even slightly decreases J_{sw}. Apparently, Joule heating, rather than the PPMS board T, has been the dominant factor of the junction temperature [33].

Limited by the equipment setup, we can only apply quasistatic currents in the T-dependent measurements with our PPMS. Ultrafast STT switching of Ta- and W-pMTJs at cryogenic T has been reported elsewhere [23], [34].

V. Conclusion

In summary, we prepared nanoscale Mo-pMTJ devices, demonstrated their ultrafast switching on a timescale down to sub-ns, and verified their cryogenic functionality down to 2 K. VSM measurements were conducted to confirm the strong PMA of the Mo-pMTJ stack. STEM characterizations show a diameter of about 100 nm and good structure integrity of patterned devices. By performing systematic P measurements, we analyzed the ultrafast switching of Mo-pMTJs with various τ and J. The switching is observed, being well within the precessional regime. The optimal E is 0.64 pJ/bit (P→AP) and 0.71 pJ/bit (AP→P), respectively. Due to the increase of R_{AP}, the TMR ratio is almost doubled when devices are cooled down to 2 K. J_{sw} generally increases as T decreases, except for deeply low T, at which the Joule heating determines the junction temperature. Our study advances Mo-pMTJ devices for their promising memory and logic applications, including the cryogenic memory in superconducting circuits.

References

[1] T. Kishi, H. Yoda, T. Kai, T. Nagase, E. Kitagawa, M. Yoshikawa, K. Nishiyama, T. Daibou, M. Nagamine, M. Amano, S. Takahashi, M. Nakayama, N. Shimomura, H. Aikawa, S. Ikegawa, S. Yuasa, K. Yakushiji, H. Kubota, A. Fukushima, M. Oogane, T. Miyazaki, and K. Ando, "Lower-current and fast switching of a perpendicular TMR for high speed and high density spin-transfer-torque MRAM," in *Proc. IEEE Int. Electron. Devices Meeting*, Dec. 2008, pp. 309–314, doi: 10.1109/IEDM.2008.4796680.

[2] Z. Diao, Z. Li, S. Wang, Y. Ding, A. Panchula, E. Chen, L.-C. Wang, and Y. Huai, "Spin-transfer torque switching in magnetic tunnel junctions and spin-transfer torque random access memory," *J. Phys., Condens. Matter*, vol. 19, no. 16, Apr. 2007, Art. no. 165209, doi: 10.1088/0953-8984/19/16/165209.

[3] K. C. Chun, H. Zhao, J. D. Harms, T.-H. Kim, J.-P. Wang, and C. H. Kim, "A scaling roadmap and performance evaluation of in-plane and perpendicular MTJ based STT-MRAMs for high-density cache memory," *IEEE J. Solid-State Circuits*, vol. 48, no. 2, pp. 598–610, Feb. 2013, doi: 10.1109/JSSC.2012.2224256.

[4] D. C. Worledge, G. Hu, D. W. Abraham, J. Z. Sun, P. L. Trouilloud, J. Nowak, S. Brown, M. C. Gaidis, E. J. O'Sullivan, and R. P. Robertazzi, "Spin torque switching of perpendicular Ta | CoFeB | MgO-based magnetic tunnel junctions," *Appl. Phys. Lett.*, vol. 98, no. 2, Jan. 2011, Art. no. 022501, doi: 10.1063/1.3536482.

[5] S. Ikeda, K. Miura, H. Yamamoto, K. Mizunuma, H. D. Gan, M. Endo, S. Kanai, J. Hayakawa, F. Matsukura, and H. Ohno, "A perpendicular-anisotropy CoFeB–MgO magnetic tunnel junction," *Nature Mater.*, vol. 9, no. 9, pp. 721–724, Jul. 2010, doi: 10.1038/nmat2804.

[6] Z. Wang, M. Saito, K. P. McKenna, S. Fukami, H. Sato, S. Ikeda, H. Ohno, and Y. Ikuhara, "Atomic-scale structure and local chemistry of CoFeB–MgO magnetic tunnel junctions," *Nano Lett.*, vol. 16, no. 3, pp. 1530–1536, Feb. 2016, doi: 10.1021/acs.nanolett.5b03627.

[7] W. C. Tsai, S. C. Liao, H. C. Hou, C. T. Yen, Y. H. Wang, H. M. Tsai, F. H. Chang, H. J. Lin, and C.-H. Lai, "Investigation of perpendicular magnetic anisotropy of CoFeB by X-ray magnetic circular dichroism," *Appl. Phys. Lett.*, vol. 100, no. 17, Apr. 2012, Art. no. 172414, doi: 10.1063/1.4707380.

[8] H. X. Yang, M. Chshiev, B. Dieny, J. H. Lee, A. Manchon, and K. H. Shin, "First-principles investigation of the very large perpendicular magnetic anisotropy at Fe | MgO and Co | MgO interfaces," *Phys. Rev. B, Condens. Matter*, vol. 84, no. 5, Aug. 2011, Art. no. 054401, doi: 10.1103/PhysRevB.84.054401.

[9] N. Miyakawa, D. C. Worledge, and K. Kita, "Impact of ta diffusion on the perpendicular magnetic anisotropy of Ta/CoFeB/MgO," *IEEE Magn. Lett.*, vol. 4, 2013, Art. no. 1000104, doi: 10.1109/LMAG.2013.2240266.

[10] G.-G. An, J.-B. Lee, S.-M. Yang, J.-H. Kim, W.-S. Chung, and J.-P. Hong, "Highly stable perpendicular magnetic anisotropies of CoFeB/MgO frames employing W buffer and capping layers," *Acta Mater.*, vol. 87, pp. 259–265, Apr. 2015, doi: 10.1016/j.actamat.2015.01.022.

[11] M. Wang, W. Cai, K. Cao, J. Zhou, J. Wrona, S. Peng, H. Yang, J. Wei, W. Kang, Y. Zhang, J. Langer, B. Ocker, A. Fert, and W. Zhao, "Current-induced magnetization switching in atom-thick tungsten engineered perpendicular magnetic tunnel junctions with large tunnel magnetoresistance," *Nature Commun.*, vol. 9, no. 1, pp. 1–7, Feb. 2018, doi: 10.1038/s41467-018-03140-z.

[12] H. Almasi, D. R. Hickey, T. Newhouse-Illige, M. Xu, M. R. Rosales, S. Nahar, J. T. Held, K. A. Mkhoyan, and W. G. Wang, "Enhanced tunneling magnetoresistance and perpendicular magnetic anisotropy in Mo/CoFeB/MgO magnetic tunnel junctions," *Appl. Phys. Lett.*, vol. 106, no. 18, May 2015, Art. no. 182406, doi: 10.1063/1.4919873.

[13] K. Watanabe, S. Fukami, H. Sato, F. Matsukura, and H. Ohno, "Magnetic properties of CoFeB–MgO stacks with different buffer-layer materials (Ta or Mo)," *IEEE Trans. Magn.*, vol. 52, no. 7, pp. 1–4, Jul. 2016, doi: 10.1109/TMAG.2016.2514525.

[14] P. J. Chen, Y. L. Iunin, S. F. Cheng, and R. D. Shull, "Underlayer effect on perpendicular magnetic anisotropy in $Co_{20}Fe_{60}B_{20}$/MgO films," *IEEE Trans. Magn.*, vol. 52, no. 7, pp. 1–4, Jul. 2016, doi: 10.1109/TMAG.2015.2511662.

[15] T. Liu, J. W. Cai, and L. Sun, "Large enhanced perpendicular magnetic anisotropy in CoFeB/MgO system with the typical Ta buffer replaced by an Hf layer," *AIP Adv.*, vol. 2, no. 3, Sep. 2012, Art. no. 032151, doi: 10.1063/1.4748337.

[16] Y.-W. Oh, K.-D. Lee, J.-R. Jeong, and B.-G. Park, "Interfacial perpendicular magnetic anisotropy in CoFeB/MgO structure with various underlayers," *J. Appl. Phys.*, vol. 115, no. 17, May 2014, Art. no. 17C724, doi: 10.1063/1.4864047.

[17] X. Li, T. Sasaki, C. Grezes, D. Wu, K. Wong, C. Bi, P.-V. Ong, F. Ebrahimi, G. Yu, N. Kioussis, W. Wang, T. Ohkubo, P. K. Amiri, and K. L. Wang, "Predictive materials design of magnetic random-access memory based on nanoscale atomic structure and element distribution," *Nano Lett.*, vol. 19, no. 12, pp. 8621–8629, Nov. 2019, doi: 10.1021/acs.nanolett.9b03190.

[18] H. Cheng, J. Chen, S. Peng, B. Zhang, Z. Wang, D. Zhu, K. Shi, S. Eimer, X. Wang, Z. Guo, Y. Xu, D. Xiong, K. Cao, and W. Zhao, "Giant perpendicular magnetic anisotropy in Mo-based double-interface free layer structure for advanced magnetic tunnel junctions," *Adv. Electron. Mater.*, vol. 6, no. 8, Aug. 2020, Art. no. 2000271, doi: 10.1002/aelm.202000271.

[19] P. Khanal, B. Zhou, M. Andrade, Y. Dang, A. Davydov, A. Habiboglu, J. Saidian, A. Laurie, J.-P. Wang, D. B. Gopman, and W. Wang, "Perpendicular magnetic tunnel junctions with multi-interface free layer," *Appl. Phys. Lett.*, vol. 119, no. 24, Dec. 2021, Art. no. 242404, doi: 10.1063/5.0066782.

[20] H. Cheng, B. Zhang, Y. Xu, S. Lu, Y. Yao, R. Xiao, K. Cao, Y. Liu, Z. Wang, R. Xu, D. Xiong, Y. Wang, H. Ma, S. Eimer, C. Zhao, and W. Zhao, "Mo-based perpendicularly magnetized thin films with low damping for fast and low-power consumption magnetic memory," *Sci. China-Phys. Mech. Astron.*, vol. 65, no. 8, Aug. 2022, Art. no. 287511. [Online]. Available: http://engine.scichina.com/doi/10.1007/s11433-021-1875-6

[21] Y. Huai, H. Gan, Z. Wang, P. Xu, X. Hao, B. K. Yen, R. Malmhall, N. Pakala, C. Wang, J. Zhang, Y. Zhou, D. Jung, K. Satoh, R. Wang, L. Xue, and M. Pakala, "High performance perpendicular magnetic tunnel junction with Co/Ir interfacial anisotropy for embedded and standalone STT-MRAM applications," *Appl. Phys. Lett.*, vol. 112, no. 9, Feb. 2018, Art. no. 092402, doi: 10.1063/1.5018874.

[22] J. Z. Sun, "Spin-current interaction with a monodomain magnetic body: A model study," *Phys. Rev. B, Condens. Matter*, vol. 62, no. 1, pp. 570–578, 2000, doi: 10.1103/PhysRevB.62.570.

[23] L. Rehm, G. Wolf, B. Kardasz, M. Pinarbasi, and A. D. Kent, "Sub-nanosecond spin-torque switching of perpendicular magnetic tunnel junction nanopillars at cryogenic temperatures," *Appl. Phys. Lett.*, vol. 115, no. 18, Oct. 2019, Art. no. 182404, doi: 10.1063/1.5128106.

[24] D. S. Holmes, A. L. Ripple, and M. A. Manheimer, "Energy-efficient superconducting computing—Power budgets and requirements," *IEEE Trans. Appl. Supercond.*, vol. 23, no. 3, Jun. 2013, Art. no. 1701610, doi: 10.1109/TASC.2013.2244634.

[25] Y. Lv and J.-P. Wang, "A single magnetic-tunnel-junction stochastic computing unit," in *IEDM Tech. Dig.*, Dec. 2017, p. 36, doi: 10.1109/IEDM.2017.8268504.

[26] K. Lee and S. H. Kang, "Control of switching current asymmetry by magnetostatic field in MgO-based magnetic tunnel junctions," *IEEE Electron Device Lett.*, vol. 30, no. 12, pp. 1353–1355, Dec. 2009, doi: 10.1109/LED.2009.2033129.

[27] H. Zhao, A. Lyle, Y. Zhang, P. K. Amiri, G. Rowlands, Z. Zeng, J. Katine, H. Jiang, K. Galatsis, K. L. Wang, I. N. Krivorotov, and J.-P. Wang, "Low writing energy and sub nanosecond spin torque transfer switching of in-plane magnetic tunnel junction for spin torque transfer random access memory," *J. Appl. Phys.*, vol. 109, no. 7, Apr. 2011, Art. no. 07C720, doi: 10.1063/1.3556784.

[28] Y. Takeuchi, H. Sato, S. Fukami, F. Matsukura, and H. Ohno, "Temperature dependence of energy barrier in CoFeB–MgO magnetic tunnel junctions with perpendicular easy axis," *Appl. Phys. Lett.*, vol. 107, no. 15, Oct. 2015, Art. no. 152405, doi: 10.1063/1.4933256.

[29] K. Cao, H. Li, W. Cai, J. Wei, L. Wang, Y. Hu, Q. Jiang, H. Cui, C. Zhao, and W. Zhao, "Low-temperature performance of nanoscale perpendicular magnetic tunnel junctions with double MgO-interface free layer," *IEEE Trans. Magn.*, vol. 55, no. 3, pp. 1–4, Mar. 2019, doi: 10.1109/TMAG.2018.2877446.

[30] S. S. Parkin, C. Kaiser, A. Panchula, P. M. Rice, B. Hughes, M. Samant, and S. H. Yang, "Giant tunnelling magnetoresistance at room temperature with MgO (100) tunnel barriers," *Nature Mater.*, vol. 3, pp. 862–867, Oct. 2004, doi: 10.1038/nmat1256.

[31] C. H. Shang, J. Nowak, R. Jansen, and J. S. Moodera, "Temperature dependence of magnetoresistance and surface magnetization in ferromagnetic tunnel junctions," *Phys. Rev. B, Condens. Matter*, vol. 58, no. 6, pp. R2917–R2920, Aug. 1998, doi: 10.1103/PhysRevB.58.R2917.

[32] S. Zhang, P. M. Levy, A. C. Marley, and S. S. P. Parkin, "Quenching of magnetoresistance by hot electrons in magnetic tunnel junctions," *Phys. Rev. Lett.*, vol. 79, no. 19, pp. 3744–3747, Nov. 1997, doi: 10.1103/PhysRevLett.79.3744.

[33] L. Rehm, G. Wolf, B. Kardasz, E. Cogulu, Y. Chen, M. Pinarbasi, and A. D. Kent, "Thermal effects in spin-torque switching of perpendicular magnetic tunnel junctions at cryogenic temperatures," *Phys. Rev. Appl.*, vol. 15, no. 3, Mar. 2021, Art. no. 034088, doi: 10.1103/PhysRevApplied.15.034088.

[34] L. Lang, Y. Jiang, F. Lu, C. Wang, Y. Chen, A. D. Kent, and L. Ye, "A low temperature functioning CoFeB/MgO-based perpendicular magnetic tunnel junction for cryogenic nonvolatile random access memory," *Appl. Phys. Lett.*, vol. 116, no. 2, Jan. 2020, Art. no. 022409, doi: 10.1063/1.5129553.